

ASYMMETRIES AND OUTFLOWS IN THE CIRCUMSTELLAR DUST OF MIRA A

A. A. CHANDLER, K. TATEBE, E. H. WISHNOW, D. D. S. HALE, AND C. H. TOWNES

Space Sciences Laboratory and Department of Physics, University of California, Berkeley, CA 94720; chandler@ssl.berkeley.edu, tatebe@ssl.berkeley.edu, wishnow@ssl.berkeley.edu, david@isi.mtwilson.edu, cht@ssl.berkeley.edu

Received 2007 May 31; accepted 2007 July 27

ABSTRACT

Asymmetries and motions in the dust shell surrounding Mira A (*o* Ceti) are reported. Measurements were taken with the UC Berkeley Infrared Spatial Interferometer (ISI), a three-element interferometer operating at 11.15 μm . At the time of these observations, it was in a linear, east-west configuration with a maximum baseline of 12 m and thus had a resolution of better than 100 mas. Three years of data (2003–2005) are presented and permit observation of the movement of dust shells over time. Fits are made to the visibility and closure-phase curves, which are then used to create one-dimensional profiles of the dust shells. Asymmetries in the circumstellar dust have been observed, and several possible explanations for these asymmetries are explored.

Subject headings: binaries: symbiotic — infrared: stars — stars: individual (Mira AB) — stars: late-type — techniques: interferometric

Online material: mpeg animation

1. INTRODUCTION

Mira AB is a mildly symbiotic binary system made up of an asymptotic giant branch (AGB) star, Mira A (*o* Ceti), and its mysterious companion, Mira B. Material is transferred through a stellar outflow from the cool, evolved star (Mira A) to its hotter companion (Mira B). The large separation (~ 600 mas) between the stars is not typical, and therefore the interaction between the stars is not as strong as those in many accreting or symbiotic binaries.

Mira A dominates the Mira AB system in the mid-infrared. At a distance of 128_{-15}^{+21} pc, derived from *Hipparcos* parallax data (Perryman et al. 1997), it is one of the closest oxygen-rich AGB stars. Mira A is the long-period variable for which a class of stars, the Mira variables, are named. These stars have luminosity periods that are on the order of about 1 yr, with Mira A having a period of about 332 days (Karovska et al. 1997). Also, this stage of stellar evolution is characterized by high mass-loss rates, from 10^{-7} to $10^{-5} M_{\odot} \text{ yr}^{-1}$ (Knapp & Morris 1985), with Mira A having a mass-loss rate of $\dot{M} = 2.0 \times 10^{-7} M_{\odot} \text{ yr}^{-1}$ (Knapp et al. 1982) or $\dot{M} = 5.8 \times 10^{-8} M_{\odot} \text{ yr}^{-1}$ (Danchi et al. 1994).

Mira variables are of particular interest because they exhibit asymmetries both in the stars and in their dust shells as they transition to the proto-planetary nebula stage. The gas and dust they emit, an estimated $0.55 M_{\odot} \text{ yr}^{-1}$ in our Galaxy (Perrin et al. 2004), is a major source of molecules in the interstellar medium. According to preliminary results from the Mira Imaging Project (Ragland et al. 2006), more than a third of Mira variables exhibit asymmetries as observed by IOTA in the near-infrared. Finally, the brightness and dust distributions tend to undergo changes in less than 1 yr, making the dust movement easy to study.

The companion adds a further degree of intrigue to this system. Even though it was discovered over 85 years ago (Aitken 1923), the specific nature of Mira B has not yet been precisely determined. It is generally agreed to be about 600 mas from the AGB star at a position angle of $\sim 108^{\circ}$. It was originally believed to be a white dwarf (Joy 1954; Reimers & Cassatella 1985; Karovska et al. 1997, 2005); however, strong arguments have been made that it is instead a low-mass main-sequence star of about $0.7 M_{\odot}$ (Ireland et al. 2007; Kastner & Soker 2004; Jura & Helfand 1984). One of the most convincing pieces of evidence

supporting the latter theory is that Mira B's luminosity is much too low, $\lesssim 1 L_{\odot}$, versus the estimated $\sim 10 L_{\odot}$ required for a white dwarf. Finally, the star has been suggested to be something in between the previous two options: a variable star with a 14 yr period (Prieur et al. 2002). The nature of the companion should not play much of a role in our analysis, because the separation between Mira A and Mira B is so large that it is likely that the companion has little influence on the system in the range we consider.

The period of this binary system is not well known but is estimated to be quite long, on the order of several centuries. Whitlock (1987) suggests that the period must be longer than 200 yr. It is also proposed to be as long as 400 yr (Baize 1980), 500 yr (Prieur et al. 2002), or 610 yr (Ireland et al. 2007). Therefore, in the three years of observations presented here, it is safe to assume that there are not any significant changes due to rotation of the system. In addition, the inclination of the system is estimated to be nearly perpendicular to our line of sight, in the range of 63° – 111° (Ireland et al. 2007; Reimers & Cassatella 1985).

1.1. Previous Measurements

The Mira AB system is well studied, and many measurements have been made at a variety of wavelengths. The dust shell around the Mira system has been previously measured with the ISI (Bester et al. 1991; Danchi et al. 1994; Lopez et al. 1997). Measurements with the ISI have also been made of the AGB star's diameter and its changes (Weiner et al. 2000, 2003). Other infrared measurements of the Mira system include those made at the Keck I telescope with the Long-Wavelength Spectrometer (LWS) camera (Ireland et al. 2007), those made with the Infrared Optical Telescope Array (IOTA; Ragland et al. 2006), those made with the Mid-Infrared Array Camera (MIRAC3) at the NASA Infrared Telescope Facility (Marengo et al. 2001), and those made with the Infrared Michelson Array (IRMA; Ridgway et al. 1992). The Mira system has also been observed at wavelengths from the radio to the X-ray and almost everything in between.

2. ISI OBSERVATIONS

We report observations using the ISI over three years, 2003–2005. The specific dates for each data set are given in Table 1.

TABLE 1
ISI OBSERVATIONS OF THE MIRA SYSTEM

Year	Date of Observation	Julian Date	Stellar Phase ^a	Average Position Angle (deg)	Δ Position Angle (deg)
2003.....	Aug–Sep average	2,452,894	0.24	272.1	9.3
	Aug 27	2,452,879	0.20	272.2	2.1
	Aug 28	2,452,880	0.20	270.2	2.7
	Sep 18	2,452,901	0.26	272.3	5.8
	Sep 19	2,452,902	0.27	270.1	2.2
	Sep 23	2,452,906	0.28	272.8	10.5
	Oct–Nov average	2,452,940	0.38	269.9	1.8
	Oct 03	2,452,916	0.31	269.3	0.84
2004.....	Nov 19	2,452,963	0.45	270.6	1.2
	Average	2,453,291	0.44	271.1	12
	Oct 06	2,453,285	0.42	270.5	3.2
	Oct 14	2,453,293	0.44	272.9	3.2
2005.....	Oct 15	2,453,294	0.45	269.8	3.0
	Average	2,453,662	0.55	273.2	5.7
	Sep 22	2,453,636	0.48	271.9	4.5
	Oct 14	2,453,658	0.54	274.9	0.65
	Nov 17	2,453,692	0.64	272.7	0.10

^a Phase information was obtained through a light curve provided by AAVSO and by assuming a period of 331.9 days. The phase is defined to be 0.0 and 1.0 when the luminosity is at maximum. Please note that the stellar phase is calculated from the visible and that there is some lag from visible to infrared maxima/minima. This is discussed in § 4.2.

The ISI, located at Mount Wilson Observatory in California, is a three-element interferometer with Pfund-type telescopes. It has 1.65 m apertures; the size was chosen such that they could fit inside standard semi-trailer trucks for ease of changing baselines. The ISI is currently operating at 11.15 μm . It employs CO₂ lasers as local oscillators for heterodyne detection and has a very narrow bandwidth of ± 2.6 GHz. The original two-element array is fully described in Hale et al. (2000), and the addition of the third telescope and the capability of measuring the closure phase are described in Hale et al. (2003). During the time of these measurements, the telescopes were in a linear east-west configuration with 4, 8, and 12 m baselines, which we will refer to as the (1–2), (2–3) and (3–1) baselines, respectively. These short, linear baselines give information up to about 11×10^5 cycles rad^{-1} , defined here as 11 spatial frequency units (SFU).

While the focus of this paper is on the dust in the Mira system, the ISI has recently undergone a change of baselines, making available higher resolution data that resolve Mira A. The ISI is currently in a triangular configuration with baselines of ~ 36 m. These high-resolution ISI data (15–35 SFU) give the portion of the visibility curve corresponding to the star itself. This configuration is optimized for the detection of asymmetries in stars. A preliminary analysis of high-resolution data (2006–2007) was made to determine the diameter for the stellar photosphere of Mira A that we will use in this analysis.

3. METHODS

The technique used for these models is very similar to the methods described in Tatebe et al. (2006), but with several upgrades. Smooth fits to the visibility and closure-phase data allow for one-dimensional profiles to be created by an inverse Fourier transform. The intensity profiles show one-dimensional projections of the two-dimensional intensity distribution. A fit to the 2006–2007 long-baseline ISI measurements provides an estimate of 46 mas for the stellar diameter at a phase of 0.80. These results correlate nicely with previous ISI measurements; Weiner et al. (2000) measured Mira A’s diameter to be 47.8 ± 0.5 mas at nearly maximum phase (0.90), and Lopez et al. (1997), although they were unable to resolve the star, estimated a photospheric diameter

of between 38 and 48 mas. It is assumed for the intensity profiles that the visibility after 16 SFU (the lowest observed spatial frequency in the high-resolution data) is due to a uniform disk star with a diameter of 46 mas. Other publications suggest that a Gaussian may better fit Mira-type stars (Ireland et al. 2004). However, the average diameter from the uniform disk fit is used in these calculations for simplicity and should be a good approximation.

The star is modeled in only one dimension; therefore, it is important to consider its position angle, or the rotation angle of the star with respect to the baseline as it passes overhead, for each epoch. By averaging data over several months, we are assuming that the relatively small changes in position angle are not important to the model. A full discussion of the tolerance of small rotations is available in § 3 of Tatebe et al. (2006), which indicates that a change in position angle of up to about 16° is permissible. Our greatest change in position angle is about 10° , as listed in Table 1; therefore, it is reasonable to make one-dimensional reconstructions of the star and the surrounding dust.

4. RESULTS

The visibility data and fits are presented in Figure 1, and the closure-phase data and fits are shown in Figure 2. Figure 3 depicts the visibility phase, free of atmospheric disturbances. It is derived from a smooth fit to the closure phase and the assumption that the visibility phase returns to zero at high frequencies (i.e., it is assumed that the star is a uniform disk). This method is fully described in Tatebe et al. (2006). The intensity profiles are separated by year in order to more clearly display the data. They are shown in Figures 4, 5, and 6 for 2003, 2004, and 2005, respectively. Figures 1–3 contain information from all three years for four sets of data. (The data from 2003 are split into two sets for analysis.) In the figures, the lines represent fits to the visibility or closure phase, the reconstructed values of the visibility phase, and finally the intensity profiles themselves. The symbols represent the ISI data.

4.1. Asymmetric Circumstellar Dust

Both 2003 data sets present a similar dust distribution; however, separation of the data sets for analysis was necessary because the data span a significant change in luminosity phase. This can be

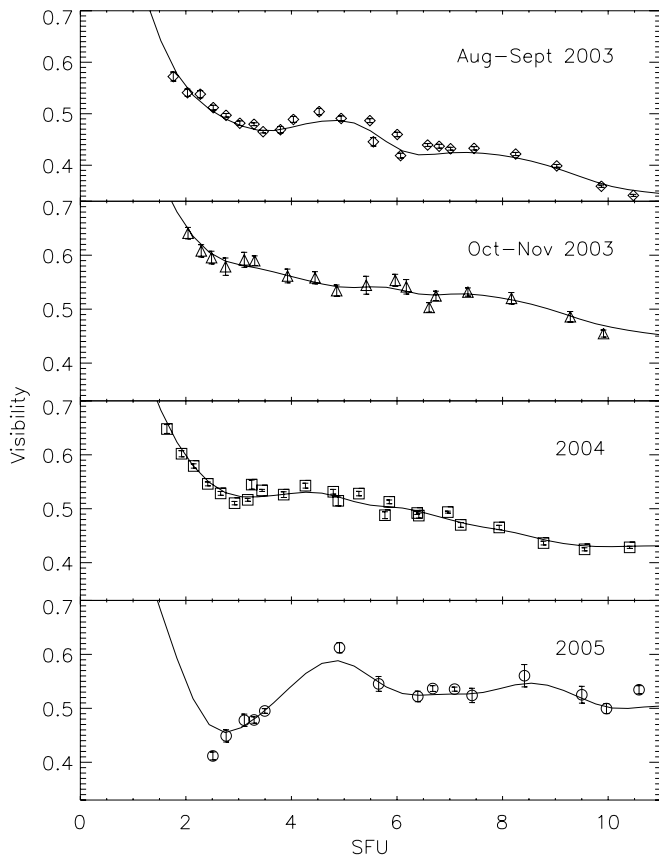


FIG. 1.—Visibility curves of Mira A. The horizontal axis is given in spatial frequency units (SFU), which are equal to 10^5 cycles rad^{-1} .

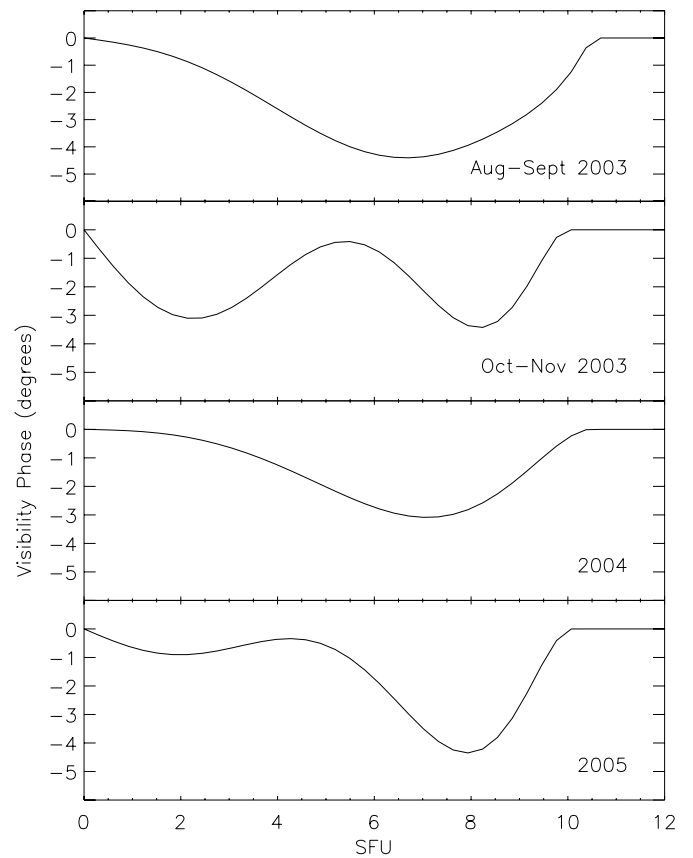


FIG. 3.—Visibility phases for Mira A, derived from closure-phase measurements.

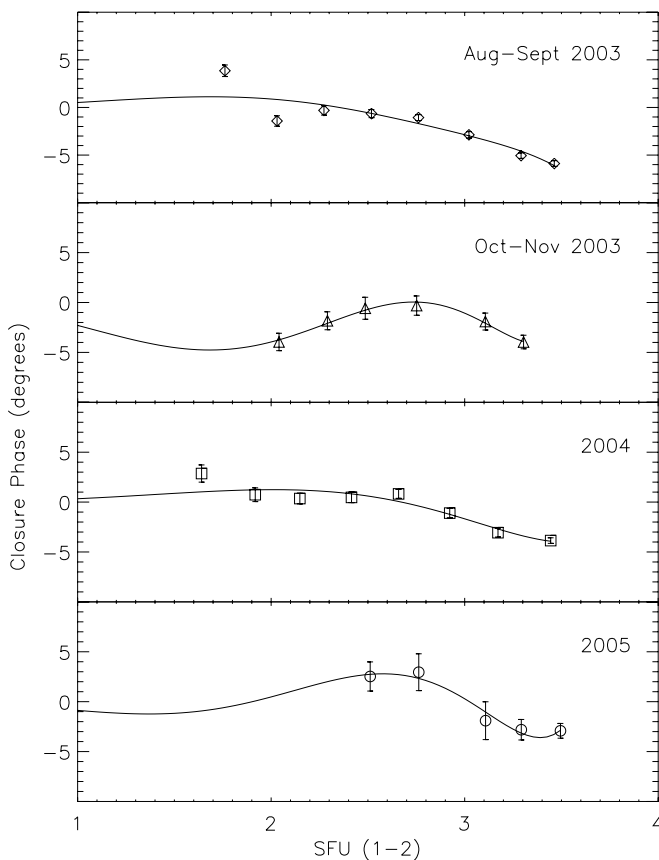


FIG. 2.—Closure-phase curves for Mira A. The horizontal axis is given in terms of SFU (1-2), or spatial frequency units as measured by the shortest baseline.

seen in Figure 1 by noting that the levels of the curves at high SFU in the first two plots differ, corresponding to different star-to-dust intensity ratios. The dust is more intense in the first epoch as compared to the second. The 2003 measurements of Mira A display a slightly negative, nonzero closure phase, indicating a small degree of asymmetry in the dust to the west. The 2003 intensity profiles can be found in Figure 4. The solid line shows the first epoch (August–September), and the dashed line shows the second (October–November). The most prominent peak in intensity from the dust

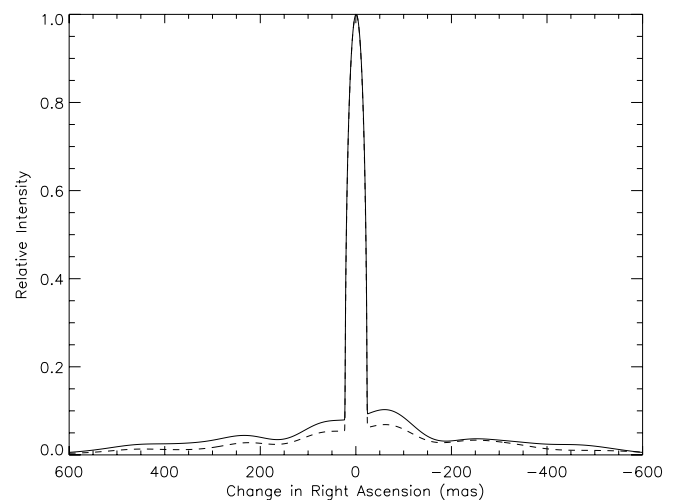


FIG. 4.—One-dimensional profile of the $11 \mu\text{m}$ intensity of Mira A. The solid line indicates the 2003 August–September data, and the dashed line represents the 2003 October–November data. The central peak is that from a uniform disk star with a diameter of 46 mas. East is to the left. This figure is included in an mpeg animation, which shows a smooth interpolation of the profiles between all four epochs, that is presented in the electronic edition of the *Journal*.

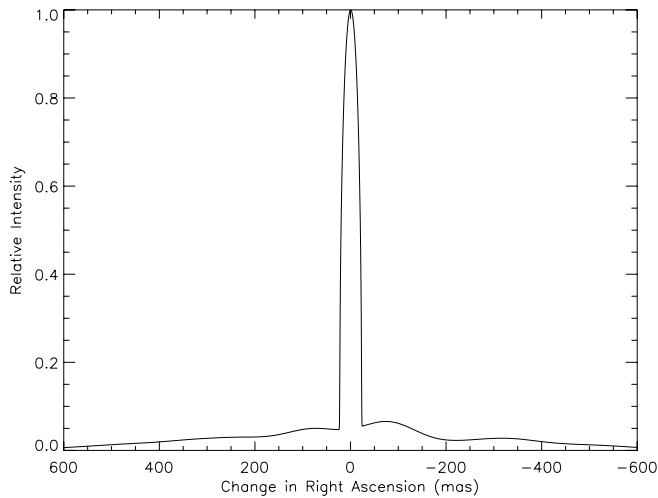


FIG. 5.—One-dimensional profile of the $11\ \mu\text{m}$ intensity of Mira A for 2004. The central peak is that from a uniform disk star with a diameter of 46 mas. East is to the left.

is at about 65 mas from the center of the star for both epochs. The intensity is slightly stronger on the west side of the star than on the east for this peak. This asymmetry is most likely caused by an asymmetry in dust concentration. Also, a secondary peak is barely visible at 233 mas to the east and 260 mas to the west.

The visibility curve for the 2004 data, at a phase close to that of the second epoch of the 2003 data, is also shown in Figure 1. The locations of the intensity peaks in the curve differ for the two years, which will be discussed in § 5.1. The closure phase is slightly negative once again, explaining the asymmetry in the dust distribution apparent in the intensity profile, which is shown in Figure 5. The asymmetry is clearly visible in the peak dust intensities, which occur at ± 80 mas from the center of the star. As was previously the case, the western peak is slightly brighter than the eastern peak. The weak, secondary peaks occur at about 250 mas to the east and 320 mas to the west.

The data change noticeably from 2003 and 2004 to 2005, as can be seen most distinctly in the visibility curve. There is a large dip at about 3 SFU, which may indicate a change in dust distribution. Also, the intensity in 2005 has smoothed out to a great degree, with the inner intensity peaks broadening to become barely visible as the largest peaks have moved out to about 240 and 320 mas in the east and west, respectively. The intensity of the dust does not change greatly over about 500 mas.

4.2. Luminosity Phase and Flux

The $11\ \mu\text{m}$ flux measured by the United Kingdom Infrared Telescope (UKIRT) was 4544 Jy at a stellar phase of 0.17 on 1989 October 30 and 4850 Jy on 1992 August 20 at a phase of 0.26 (Danchi et al. 1994). The peak $11\ \mu\text{m}$ radiation usually occurs at a visible stellar phase of ~ 0.20 , as shown by Creech-Eakman (1997), and as shown by a comparison of AAVSO data and $12\ \mu\text{m}$ photometry obtained from DIRBE on the *COBE* satellite. Mira A also takes longer to dim from maxima than to brighten from minima in the mid-infrared; hence, the minimum occurs at a visible phase of ~ 0.7 , as opposed to 0.5, as would be the case for sinusoidal variation. Therefore, the visible phases do not accurately reflect what is seen in the mid-infrared. It is likely that the measurements of visibility listed in Table 1 for 2003 are close to the peak $11\ \mu\text{m}$ flux and that for 2004 and 2005 they are a little past this peak. It must be noted that the amount of dust emitted and the infrared flux vary somewhat from cycle to cycle, so a precise comparison of

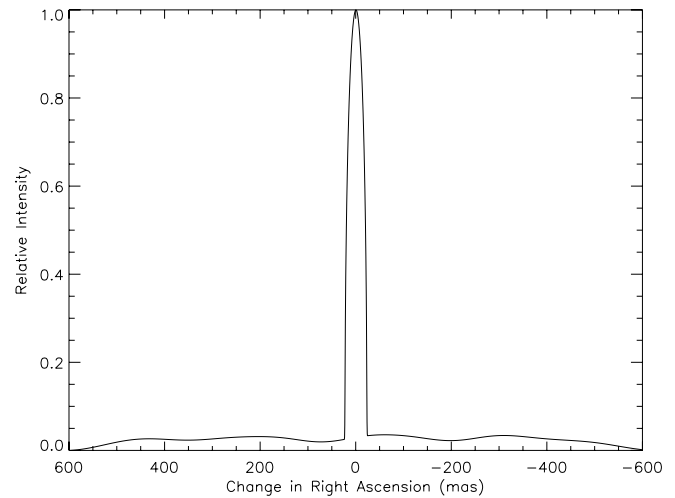


FIG. 6.—Same as Fig. 5, but for the 2005 data.

phases and fluxes between the different years cannot be made. It is assumed, however, that they are not very different for the three years reported here.

5. DISCUSSION

The ISI has made several previous measurements of the dust surrounding Mira A (Bester et al. 1991; Danchi et al. 1994; Lopez et al. 1997). Despite the roughly 10 yr period between these measurements and those presented here, the inner radius of the dust shell is consistently observed to be ~ 50 mas. Asymmetries in the dust surrounding Mira A have also been observed by Marengo et al. (2001) and Karovska et al. (1997). Measurements have been made at a variety of other wavelengths. Matthews & Karovska (2006) note an elongation along a position angle of 120° (corresponding to 300° in our system, as we measure from east to west) in the radio, confirming the X-ray elongation proposed in Karovska et al. (2005). These elongations are consistent with the brighter dust to the west of the star, as can be seen in Figures 4 and 5. A significant X-ray event in 2003 was observed in the system by Karovska et al. (2005). They suggest that if the event observed was a mass ejection, it should cool down enough by 2004–2005 to show a significant increase in dust production. The data for 2005 do not show a large increase in dust, but do show a rather different distribution from the previous years.

5.1. Dust Outflow

The innermost, primary dust intensity peak moves markedly from 2003 to 2004. In 2004 it is ~ 15 mas further from the star than in the previous year. If we assume the *Hipparcos* distance of 128 pc calculated in § 1, a change of 15 mas over 1 yr leads to an outflow rate of $9.1\ \text{km s}^{-1}$.

The secondary peaks are slightly harder to track because they are not very intense, and larger errors should be associated with these values. To the east in the 2003 plots in Figure 4, there is a peak (barely visible on linear scales) at about 235 mas. The same peak appears to have moved out 15 mas to 250 mas in the 2004 plot in Figure 5. This gives the same outflow rate as that for the primary peak ($9.1\ \text{km s}^{-1}$). It is reasonable to believe that dust outflow is indeed responsible for this change.

The peak to the west is quite puzzling, because if the change from 2003 to 2004 was caused by dust outflow, the dust would have been required to move exceptionally quickly. In 2003 the peak is at 260 mas to the west, as seen in Figure 4; in 2004 the peak lies at 320 mas to the west, as shown in Figure 5, making a

difference of 60 mas yr^{-1} or 48.8 km s^{-1} . That speed is much too fast and may be in error because of the low intensity and broad nature of this peak. Alternately, perhaps dust outflow is not the best way to describe this change. It is possible that the manner in which the star illuminates the dust changed from 2003 to 2004 on the western side of the star.

Previous measurements of the outflow velocity tend to be slightly lower; for example, Bowers & Knapp (1988) find an outflow of 4.6 km s^{-1} from H I emission. However, they assume a distance of 77 pc to the star. If it is converted to an angular velocity, the outflow rate becomes 12.5 mas yr^{-1} , which agrees relatively well with our value. Knapp et al. (1982) used the CO(2–1) line to measure a slightly faster outflow velocity of $4.9 \pm 0.8 \text{ km s}^{-1}$. Both velocities (Bowers & Knapp 1988; Knapp et al. 1982) were calculated from Doppler broadening and therefore measure the outflow of the gas, as opposed to the dust, which is measured in the current work. The dust likely moves faster than the gas because dust is accelerated by the stellar radiation pressure. Furthermore, Ireland et al. (2007) state that the outflow rate from Mira-type stars tends to be $< 10 \text{ km s}^{-1}$; therefore, our calculation for the wind is quite typical for such stars.

If we assume that the outflow rate is 15 mas yr^{-1} , as calculated above, and that the distance between the primary and secondary shells is about 170–190 mas, a shell is emitted every 11–12 yr, or every 12–13 pulsation cycles of the star. If shells are emitted at a frequency higher than every 3–5 yr, the ISI would not be able to detect the differences between shells; it would presumably look like a continuum. Therefore, it is possible that shells are being emitted more frequently, with brighter shells being emitted on the order of every decade.

5.2. The Companion: Mira B

It seems that the companion does not have any great effect on the dust profile. Tatebe et al. (2006) discuss a close binary system and a possible shift of the central dust peak in the direction of the companion such that the star was not in the center of the dust peak. This type of asymmetry is not present here. The companion in the binary system considered in that work (R Aquarii) is, however, at least an order of magnitude closer to its primary than is Mira B. Whitelock (1987) and Ragland et al. (2006) suggest that the Mira AB system is only mildly symbiotic due to its large separation (about 600 mas). Therefore, Mira B seems to be far enough away to not have a significant effect on the dust within 500 mas of the star. While it is apparent from the intensity profiles presented here that the companion (Mira B) does not affect the dust very near Mira A, it most likely plays a role farther out. A third element in the system has also been suggested (Baize 1980; Prieur et al. 2002; Ireland et al. 2007); however, we did not find any evidence to support that possibility.

5.3. Possible Sources of Asymmetry

As a pulsating variable, Mira A has several internal means of generating asymmetry. For example, Mira A is affected by shock waves formed by the pulsation process (Karovska et al. 1997). The nature of these shock waves is not well known and could affect the process through which dust is formed around the star. Other properties, such as the magnetic field of the star, could also shape the distribution of the dust.

It seems that for Mira A, the asymmetry comes from nonuniform formation of dust. In addition, the amount of dust given off varies with time; i.e., the amount of dust emitted per year changes, creating shells of different intensities. Finally, it is quite possible that the mechanisms that illuminate the dust vary over time.

TABLE 2
UNCERTAINTIES IN VISIBILITY CALIBRATION AND CLOSURE-PHASE ZERO

Year	Baseline (1-2) (%)	Baseline (2-3) (%)	Baseline (3-1) (%)	Closure Phase (deg)
2003.....	2.7	3.8	2.3	± 1.10
2004.....	1.8	1.1	1.2	± 1.10
2005.....	1.6	1.7	3.2	± 0.72

5.4. Possible Errors

There are several places in which errors might be affecting our analysis. Table 2 shows the errors in the data calibrations. The uncertainty in the visibility data is given as a percentage, and the error in the closure-phase zero is given in units of degrees. A change in either of these values results only in small shifts of the curves (visibility or closure phase) up or down on the y -axis. The small errors, up to 4% in visibility or $\pm 1.1^\circ$ in closure phase, should not greatly affect the general structure of the results.

The final fit is chosen to be as smooth as possible, in line with the philosophy of other widely used methods, such as the maximum entropy method (MEM), and to prevent negative intensities in the model. Many other options are available for the fits; e.g., it could be more bumpy and fit every point, or it could be smoother and not fit the points as well. However, as described in Tatebe et al. (2006), changes in the fit to the visibility curve do not cause large differences in the profile. The main components remain the same regardless.

Several assumptions are employed in order to make the profiles. Mira A is assumed to be spherically symmetric, and the dust around it is assumed to be optically thin enough to allow the observation of radiation from the star itself. An asymmetric star will have little effect on the profiles, only slightly changing the central peak. Finally, we assume that the phase is smooth. This too seems to be a good approximation, as it is consistent with our measurements and earlier data. Therefore, overall, the assumptions that we have made all seem to represent the data well.

6. CONCLUSION

Mira A is surrounded by an asymmetrical distribution of dust. The brightest dust peaks are relatively near the star, but they are moving outward at about 15 mas yr^{-1} or 9.1 km s^{-1} . Less intense peaks, 200–300 mas from the star, suggest periodic emission of dust with a frequency on the order of 10 yr.

The role of the companion in this system is still unknown. It seems that Mira B is too far from Mira A to cause a significant change in the dust distribution on a scale of 500 mas from the star. Also, the excess dust emission is on the side opposite to Mira B, suggesting that some other mechanism is responsible for the asymmetry. The most likely explanations for the asymmetry in the dust distribution are asymmetric emission or illumination.

We appreciate *Hipparcos* and *ISO* data obtained from the SIMBAD database and are thankful for data obtained from the AAVSO database. We used the DIRBE Point-Source Photometry Research Tool, provided by LAMBDA at NASA's Goddard Space Flight Center. Also, we are extremely grateful for support from the Office of Naval Research, the National Science Foundation, and the Gordon and Betty Moore Foundation. Finally, we would like to thank Walt Fitelson for his invaluable contributions to keeping the ISI running.

REFERENCES

- Aitken, R. G. 1923, *PASP*, 35, 323
Baize, P. 1980, *A&AS*, 39, 83
Bester, M., Danchi, W. C., Degiacomi, C. G., Townes, C. H., & Geballe, T. R. 1991, *ApJ*, 367, L27
Bowers, P. F., & Knapp, G. R. 1988, *ApJ*, 332, 299
Creech-Eakman, M. J. 1997, Ph.D. thesis, Univ. Denver
Danchi, W. C., Bester, M., Degiacomi, C. G., Greenhill, L. J., & Townes, C. H. 1994, *AJ*, 107, 1469
Hale, D. D. S., Fitelson, W., Monnier, J. D., Weiner, J., & Townes, C. H. 2003, *Proc. SPIE*, 4838, 387
Hale, D. D. S., et al. 2000, *ApJ*, 537, 998
Ireland, M. J., Tuthill, P. G., Bedding, T. R., Robertson, J. G., & Jacob, A. P. 2004, *MNRAS*, 350, 365
Ireland, M. J., et al. 2007, *ApJ*, 662, 651
Joy, A. H. 1954, *ApJS*, 1, 39
Jura, M., & Helfand, D. J. 1984, *ApJ*, 287, 785
Karovska, M., Hack, W., Raymond, J., & Guinan, E. 1997, *ApJ*, 482, L175
Karovska, M., Schlegel, E., Hack, W., Raymond, J. C., & Wood, B. E. 2005, *ApJ*, 623, L137
Kastner, J. H., & Soker, N. 2004, *ApJ*, 616, 1188
Knapp, G. R., & Morris, M. 1985, *ApJ*, 292, 640
Knapp, G. R., Phillips, T. G., Leighton, R. B., Lo, K. Y., Wannier, P. G., Wootten, H. A., & Huggins, P. J. 1982, *ApJ*, 252, 616
Lopez, B., et al. 1997, *ApJ*, 488, 807
Marengo, M., Karovska, M., Fazio, G. G., Hora, J. L., Hoffmann, W. H., Dayal, A., & Deutsch, L. K. 2001, *ApJ*, 556, L47
Matthews, L. D., & Karovska, M. 2006, *ApJ*, 637, L49
Perrin, G., et al. 2004, *A&A*, 426, 279
Perryman, M. A. C., et al. 1997, *A&A*, 323, L49
Priour, J. L., Aristidi, E., Lopez, B., Scardia, M., Mignard, F., & Carbillet, M. 2002, *ApJS*, 139, 249
Ragland, S., et al. 2006, *ApJ*, 652, 650
Reimers, D., & Cassatella, A. 1985, *ApJ*, 297, 275
Ridgway, S. T., Benson, J. A., Dyck, H. M., Townsley, L. K., & Hermann, R. A. 1992, *AJ*, 104, 2224
Tatebe, K., Chandler, A. A., Hale, D. D. S., & Townes, C. H. 2006, *ApJ*, 652, 666
Weiner, J., Danchi, W. C., Hale, D. D. S., McMahon, J., Townes, C. H., Monnier, J. D., & Tuthill, P. G. 2000, *ApJ*, 544, 1097
Weiner, J., Hale, D. D. S., & Townes, C. H. 2003, *ApJ*, 588, 1064
Whitelock, P. A. 1987, *PASP*, 99, 573